2009 American Control Conference
Hyatt Regency Riverfront, St. Louis, MO, USA
June 10-12, 2009

Model Predictive Control of Film Porosity in Thin Film Deposition

Gangshi Hu, Gerassimos Orkoulas and Panagiotis D. Christofides

***Abstract*— A model predictive controller is developed to regulate film porosity and minimize its fluctuation in thin film deposition. The deposition process is modeled via kinetic Monte Carlo (kMC) simulation on a triangular lattice. The microscopic events involve atom adsorption and migration and allow for vacancies and overhangs to develop. Appropriate definitions of film site occupancy ratio (SOR), i.e., fraction of film sites occupied by particles over total number of film sites, and its fluctuation are introduced to describe film porosity. Deterministic and stochastic ordinary differential equation (ODE) models are also constructed to describe the time evolution of film SOR and its fluctuation. The coefficients of the ODE models are estimated on the basis of data obtained from the kMC simulator of the deposition process using least-square methods. The developed ODE models are used as the basis for the design of model predictive control (MPC) algorithms that include penalty on the film SOR and its variance to regulate the expected value of film SOR at a desired level and reduce run-to-run fluctuations. Simulation results demonstrate the applicability and effectiveness of the proposed film porosity control method in the context of the deposition process under consideration.**

I. INTRODUCTION

Currently, there is an increasing need to improve semiconductor manufacturing process operation and yield. This need has arisen due to the increased complexity and density of devices on the wafer, which is the result of increased wafer size and smaller device dimensions. Within this manufacturing environment, thin film porosity has emerged as an important film quality variable which strongly influences the electrical and mechanical properties of microelectronic devices. For example, low-κ dielectric films of high porosity are being used in current interconnect technologies to meet resistive-capacitive delay goals and minimize cross-talk. However, increased porosity negatively affects the mechanical properties of dielectric films, increasing the risk of thermo-mechanical failures [11]. Furthermore, in the case of gate dielectrics, it is important to reduce thin film porosity as much as possible and eliminate the development of holes close to the interface.

Two fundamental modeling approaches, kinetic Monte Carlo (kMC) methods [5], [6], [12], [22] and stochastic differential equation (SDE) models [3], [4], [21], have been developed to describe the evolution of film microscopic configurations and design feedback control laws. Specifically, kMC models were initially used to develop a methodology for modeling and feedback control of thin film surface roughness [2], [13], [14]. For example, a method that couples partial differential equation (PDE) models and kMC models was developed for computationally efficient multiscale optimization of thin film growth [20]. However, kMC models are not available in closed-form and this limitation precludes the use of kMC models for system-level analysis and model-based feedback control design. SDEs arise naturally in the modeling of surface morphology of ultra thin films since they can contain the surface morphology information and account for the stochastic nature of the growth processes.

Advanced control methods based on SDEs have been developed to address the need of model-based feedback control of thin film surface roughness. Specifically, methods for state feedback control of surface roughness based on linear [15], [19] and nonlinear [16], [17] SDE models have been developed. More recently, output feedback control of surface roughness was developed [7] by incorporating a Kalman-Bucy type filter. Despite recent significant efforts on surface roughness control, a close study of the existing literature indicates the lack of general and practical methods for addressing the challenging issue of achieving desired electrical and mechanical thin film properties by controlling film porosity to a desired level and reducing run-to-run porosity variability.

Motivated by above, the present work focuses on the development of model predictive control of film porosity in thin film deposition processes. A thin film deposition process which involves atom adsorption and migration is introduced and is modeled using a triangular lattice-based kMC simulator. Appropriate definitions of film site occupancy ratio (SOR) and its fluctuation are introduced to describe film porosity. Then, deterministic and stochastic ODE models are derived that describe the time evolution of film SOR and its fluctuation, and their coefficients are estimated from data obtained from the kMC simulator. The developed ODE models are used as the basis for the design of model predictive control (MPC) algorithms that include penalty on the film SOR and its variance to regulate the expected value of film SOR at a desired level and reduce run-to-run fluctuations. The MPC algorithms are applied to the kMC simulator of the deposition process and the closed-loop performance is evaluated.

II. THIN FILM DEPOSITION PROCESS DESCRIPTION AND MODELING

This section is associated with the description of the deposition process and its simulation via kMC algorithms.

Gangshi Hu and Gerassimos Orkoulas are with the Department of Chemical and Biomolecular Engineering, University of California, Los Angeles, CA 90095 USA.

Panagiotis D. Christofides is with the Department of Chemical and Biomolecular Engineering and the Department of Electrical Engineering, University of California, Los Angeles, CA 90095 USA.

Panagiotis D. Christofides is the corresponding author: Tel: +1(310)794-1015; Fax: +1(310)206-4107; e-mail: pdc@seas.ucla.edu.

Financial support from NSF, CBET-0652131, is gratefully acknowledged.

978-1-4244-4524-0/09/$25.00 ©2009 AACC

A. On-lattice kinetic Monte Carlo model of film growth

The thin film growth process considered in this work includes two microscopic processes: an adsorption process, in which particles are incorporated into the film from the gas phase, and a migration process, in which surface particles move to adjacent sites [12], [22], [23]. A ballistic deposition model is chosen to simulate the evolution of film porosity, which allows vacancies and overhangs to model the microstructural defects in the thin film.

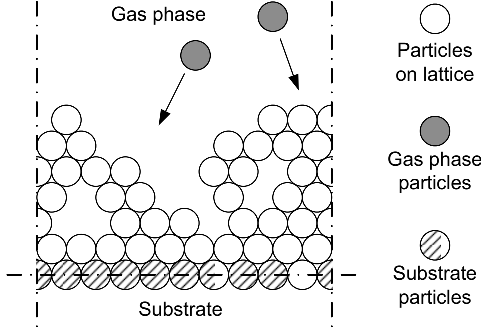

Fig. 1. Thin film growth process on a triangular lattice.

The film growth model used in this work is an on-lattice kMC model in which all particles occupy discrete lattice sites. The on-lattice kMC model is valid for temperatures $T < 0.5T_m$, where T_m is the melting point of the crystal. In this work, a triangular lattice is selected to represent the crystalline structure of the film, as shown in Fig.1. All particles are modeled as identical hard disks and the centers of the particles deposited on the film are located on the lattice sites. The diameter of the particles equals the distance between two neighboring sites. The width of the lattice is fixed so that the lattice contains a fixed number of sites in the lateral direction. The new particles are always deposited from the top side of the lattice where the gas phase is located; see Fig.1. Particle deposition results in film growth in the direction normal to the lateral direction. The direction normal to the lateral direction is thus designated as the growth direction. The number of sites in the lateral direction is defined as the lattice size and is denoted by L. The lattice parameter, a, which is defined as the distance between two neighboring sites and equals the diameter of a particle, determines the lateral extent of the lattice, La.

The number of nearest neighbors of a site ranges from zero to six, the coordination number of the triangular lattice. A site with no nearest neighbors indicates an unabsorbed particle in the gas phase (i.e., a particle which has not been deposited on the film yet). A particle with six nearest neighbors is associated with an interior particle that is fully surrounded by other particles and cannot migrate. A particle with one to five nearest neighbors is possible to diffuse to an unoccupied neighboring site with a probability that depends on its local environment.

In the simulation, a bottom layer in the lattice is initially set to be fully packed and fixed, as shown in Fig.1. There are no vacancies in this layer and the particles in this layer cannot migrate. This layer acts as the substrate for the deposition and is not counted in the computation of the number of the deposited particles, i.e., this fixed layer does not influence the film porosity (see section V-A below).

Two types of microscopic processes (Monte Carlo events) are considered, an adsorption process and a migration process. These Monte Carlo events are assumed to be Poisson processes. All events occur randomly with probabilities proportional to their respective rates. The events are executed instantaneously upon selection and the state of the lattice remains unchanged between two consecutive events.

B. Adsorption process

In an adsorption process, an incident particle comes in contact with the film and is incorporated onto the film. The microscopic adsorption rate, W, which is in units of layers per unit time, depends on the gas phase concentration. The layers in the unit of adsorption rate are densely packed layers, which contain L particles. With this definition, W is independent of L. In this work, the microscopic adsorption rate, W, is treated as a process parameter. For the entire deposition process, the macroscopic adsorption rate in terms of incident particles per unit time, which is denoted as r_a, is related to W as follows:

$$r_a = LW \tag{1}$$

The incident particles are initially placed at random positions above the film lattice and move toward the lattice in random directions. The initial particle position is uniformly distributed in the continuous domain, (0, La). The incident angle is defined as the angle between the incident direction and the direction normal to the film. The probability distribution of the incident angle is uniform in the interval (-0.5π, 0.5π).

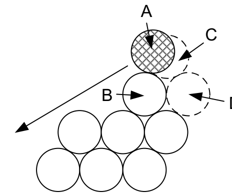

Fig. 2. Schematic of the adsorption event with surface relaxation. In this event, particle A is the incident particle, particle B is the surface particle that is first hit by particle A, site C is the nearest vacant site to particle A among the sites that neighbor particle B, and site D is a stable site where particle A relaxes.

The procedure of an adsorption process is illustrated in Fig.2. After the initial position and incident angle are determined, the incident particle, A, travels along a straight line towards the film until contacting the first particle, B, on the film. Upon contact, particle A stops and sticks to particle B at the contacting position; see Fig.2. Then, particle A moves (relaxes) to the nearest vacant site, C, among the neighboring sites of particle B. Instantaneous particle surface relaxation is conducted since site C has only one neighboring particle

and is considered unstable in the triangular lattice, as shown in Fig.2. When a particle is subject to surface relaxation, the particle moves to its most stable neighboring vacant site, which is defined as the site with the most nearest neighbors. In the case of multiple neighboring vacant sites with the same number of nearest neighbors, a random one is chosen from these sites with equal probability as the objective of the particle surface relaxation process. Note that particle surface relaxation is considered as part of the deposition event, and thus, it does not contribute to the process simulation time. There is also only one relaxation event per incident particle.

C. Migration process

In a migration process, a particle overcomes the energy barrier of the site and jumps to its vacant neighboring site. The migration rate (probability) of a particle follows an Arrhenius-type law with a pre-calculated activation energy barrier that depends on the local environment of the particle, i.e., the number of the nearest neighbors of the particle chosen for a migration event. The migration rate of the *i*th particle is calculated as follows:

$$r_{m,i} = \nu_0 \exp\left(-\frac{n_i E_0}{k_B T}\right) \tag{2}$$

where ν_0 denotes the pre-exponential factor, n_i is the number of the nearest neighbors of the *i*th particle and can take the values of 2, 3, 4 and 5 ($r_{m,i}$ is zero when $n_i = 6$ since this particle is fully surrounded by other particles and cannot migrate), E_0 is the contribution to the activation energy barrier from each nearest neighbor, k_B is the Boltzmann's constant and T is the substrate temperature of the thin film. Since the film is thin, the temperature is assumed to be uniform throughout the film and is treated as a time-varying but spatially-invariant process parameter. In this work, the factor and energy barrier contribution in Eq.2 take the following values $\nu_0 = 10^{13}\text{s}^{-1}$ and $E_0 = 0.6$ eV, which are appropriate for a silicon film [10].

When a particle is subject to migration, it can jump to either of its vacant neighboring sites with equal probability, unless the vacant neighboring site has no nearest neighbors, i.e., the surface particle cannot jump off the film and it can only migrate on the surface.

D. Simulation algorithm

To simulate the process with limited-size lattice and reduce the boundary effects, periodic boundary conditions (PBCs) are applied to the kMC model of the deposition process. With the assumption that all microscopic processes are Poisson processes, the time increment upon the execution of a successful event is computed based on the total rates of all the micro-processes, which can be listed and calculated from the current state of the lattice. To further improve the computational efficiency, a grouping algorithm is also used in the selection of the particle that is subject to migration [18]. In the grouping algorithm, the events are pre-grouped to improve the execution speed. In this work, the layer of the film emerges as a natural grouping criterion, i.e., all particles in the same layer are considered to be part of one group.

III. ODE MODELS FOR COMPLETE AND PARTIAL FILM SITE OCCUPANCY RATIO

For control purposes, dynamic models are required that describe how the film porosity expressed in terms of complete and partial film SOR varies with respect to potential manipulated input variables like temperature and deposition rate. In this section, deterministic and stochastic linear ODE models are derived to describe the evolution of film SOR. The derivation of these ODE models and the computation of their parameters is done on the basis of data obtained from the kMC model of the deposition process.

A. Definition of complete and partial film site occupancy ratios

Since film porosity is the main objective of modeling and control design of this work, complete film site occupancy ratio (SOR) is introduced to represent the extent of the porosity inside the thin film as follows:

$$\rho = \frac{N}{LH} \tag{3}$$

where ρ denotes the film SOR, N is the total number of deposited particles on the lattice, L is the lattice size (i.e., number of sites in one layer), and H denotes the number of deposited layers. At the beginning of the deposition process when there are no particles deposited on the lattice and only the substrate layer is present, a zero value is assigned to the film SOR at this state.

Another concept of film SOR introduced in this section, termed partial film SOR, is the film SOR calculated by accounting only for the top H_p layers of the film; this concept will be used to address the porosity variance reduction problem. Mathematically, the partial film SOR is defined as follows:

$$\rho_p = \frac{N_p}{LH_p} \tag{4}$$

where ρ_p denotes the partial film SOR and N_p denotes the number of particles in the top H_p layers and H_p denotes the number of top layers of the film included in the computation of the partial film SOR. Specifically, H_p fully-packed substrate layers are assumed to exist in the film before the deposition process begins and are used in the calculation of ρ_p when not enough layers have been deposited, i.e., $H < H_p$.

Although complete film SOR and partial film SOR are defined similarly, they are different variables which are used to describe different aspects of the film. The cumulative property of the complete film SOR averages the fluctuations of the porosity from different layers of the film and results in the decay of the variance of the complete film SOR to zero with respect to time. The partial film SOR, on the contrary, only accounts for the porosity of the newly deposited H_p layers of the film and the variance of the partial film SOR does not decay with respect to time. Therefore, the variance of ρ_p is selected to represent the porosity fluctuations and is used for modeling and control design. The partial film SOR variance, $\text{Var}(\rho_p)$, is computed by the following expression

$$\text{Var}(\rho_p) = \left\langle (\rho_p - \langle \rho_p \rangle)^2 \right\rangle \tag{5}$$

where $\langle\cdot\rangle$ denotes the average (mean) value.

B. Deterministic and stochastic dynamic models

The dynamics of the expected values of the complete and partial film SORs evolution can be approximately described by first-order deterministic and stochastic ODE models, respectively. A linear first-order deterministic ODE is chosen to describe the dynamics of the complete film SOR as follows:

$$\tau \frac{d\langle\rho(t)\rangle}{dt} = \rho^{ss} - \langle\rho(t)\rangle \tag{6}$$

where τ is the time constant and ρ^{ss} is the steady-state value of the complete film SOR. The model parameters, τ and ρ^{ss}, depend on substrate temperature. This dependence will be mathematically expressed in section III-C below. The deterministic ODE system of Eq.8 is subject to the following initial condition:

$$\langle\rho(t_0)\rangle = \rho_0 \tag{7}$$

where t_0 is the initial time and ρ_0 is the initial value of the complete film SOR ($\rho_0 = 0$ by convention in this work). From Eqs.6 and 7, it follows that

$$\langle\rho(t)\rangle = \rho^{ss} + (\rho_0 - \rho^{ss})\, e^{-(t-t_0)/\tau}. \tag{8}$$

A linear stochastic ODE is used to model the dynamics of the partial film SOR. Similarly to the deterministic ODE model for the expected complete film SOR of Eq.6, a first-order stochastic ODE is chosen for the computation of the partial film SOR as follows:

$$\tau_p \frac{d\rho_p(t)}{dt} = \rho_p^{ss} - \rho_p(t) + \xi_p(t) \tag{9}$$

where ρ_p^{ss} and τ_p are the two model parameters which denote the steady-state value of the partial film SOR and the time constant, respectively, and $\xi_p(t)$ is a Gaussian white noise with the following expressions for its mean and covariance:

$$\begin{aligned} \langle\xi_p(t)\rangle &= 0 \\ \langle\xi_p(t)\xi_p(t')\rangle &= \sigma_p^2\delta(t-t') \end{aligned} \tag{10}$$

where σ_p is a parameter which measures the intensity of the Gaussian white noise and $\delta(\cdot)$ denotes the standard Dirac delta function. The model parameters ρ_p^{ss}, τ_p and σ_p are functions of the substrate temperature.

The stochastic ODE system of Eq.9 is subject to the following initial condition:

$$\rho_p(t_0) = \rho_{p0} \tag{11}$$

where ρ_{p0} is the initial value of the partial film SOR. Note that ρ_{p0} is a random number, which follows a Gaussian distribution.

The following analytical solution of Eq.9 can be obtained from a direct computation as follows:

$$\rho_p(t) = \rho_p^{ss} + \left(\rho_{s0} - \rho_p^{ss}\right) e^{-(t-t_0)/\tau_p} + \int_{t_0}^{t} e^{-(s-t_0)/\tau_p}\xi_s ds. \tag{12}$$

In Eq.12, $\rho_p(t)$ is a random process, the expected value of which, $\langle\rho_p(t)\rangle$, can be obtained as follows:

$$\langle\rho_p(t)\rangle = \rho_p^{ss} + \left(\langle\rho_{s0}\rangle - \rho_p^{ss}\right) e^{-(t-t_0)/\tau_p}. \tag{13}$$

The analytical solution of $\mathrm{Var}(\rho_p)$ can be obtained from the solution of Eq.12 using the following result [1]:

Result 1: If (1) $f(x)$ is a deterministic function, (2) $\eta(x)$ is a random process with $\langle\eta(x)\rangle = 0$ and covariance $\langle\eta(x)\eta(x')\rangle = \sigma^2\delta(x-x')$, and (3) $\varepsilon = \int_a^b f(x)\eta(x)dx$, then ε is a real random variable with $\langle\varepsilon\rangle = 0$ and variance $\langle\varepsilon^2\rangle = \sigma^2\int_a^b f^2(x)dx$.

Using Result 1, the variance of the partial film SOR, $\mathrm{Var}(\rho_p)$, can be obtained from the analytical solution of Eq.12 as follows:

$$\mathrm{Var}(\rho_p(t)) = \frac{\tau_p\sigma_p^2}{2} + \left(\mathrm{Var}(\rho_{p0}) - \frac{\tau_p\sigma_p^2}{2}\right) e^{-2(t-t_0)/\tau_p} \tag{14}$$

where $\mathrm{Var}(\rho_{p0})$ is the variance of the partial film SOR at time $t = 0$, which is calculated as follows:

$$\mathrm{Var}(\rho_{p0}) = \left\langle(\rho_{p0} - \langle\rho_{p0}\rangle)^2\right\rangle. \tag{15}$$

A new model parameter, Var_p^{ss}, is introduced to simplify the solution of $\mathrm{Var}(\rho_p)$ in Eq.14 as follows:

$$\mathrm{Var}_p^{ss} = \frac{\tau_p\sigma_p^2}{2} \tag{16}$$

where Var_p^{ss} stands for the steady-state value of the variance of the partial film SOR. With the introduction of this new model parameter, the solution of the variance of the partial film SOR, $\mathrm{Var}(\rho_p)$, can be rewritten in the following form:

$$\mathrm{Var}(\rho_p(t)) = \mathrm{Var}_p^{ss} + \left(\mathrm{Var}(\rho_{p0}) - \mathrm{Var}_p^{ss}\right) e^{-2(t-t_0)/\tau_p}. \tag{17}$$

C. Parameter estimation and dependence on the process parameters

Since the ODE models of Eqs.6 and 9 are linear, the five parameters, ρ^{ss}, τ, ρ_p^{ss}, τ_p and Var_p^{ss}, can be estimated from the solutions of Eqs.8 and 13. Specifically, the parameters ρ_p^{ss} and τ_p are estimated using Eq.8 and the parameters ρ_p^{ss}, τ_p and Var_p^{ss} are estimated using Eq.13, solving two separate least square problems. Specifically, the two least-square problems can be solved independently to obtain the first four model parameters. The steady-state variance, Var_p^{ss}, is obtained from the steady-state values of the variance evolution profiles at large times.

The data used for the parameter estimation are obtained from the open-loop kMC simulation of the thin film growth process. The process parameters are fixed during each open-loop simulation so that the dependence of the model parameters on the process parameters can be obtained for fixed operation conditions. The complete film SOR and the partial film SOR are calculated on the basis of the deposited film at specific time instants. Due to the stochastic nature of the process, multiple independent simulation runs are performed to obtain the expected values of the complete film SOR and of the partial film SOR as well as of the variance of the partial film SOR. Details of the modeling results can be found in [9].

IV. Model predictive control design

In this section, we design model predictive controllers based on the deterministic and stochastic ODE models of Eqs.6 and 9 to simultaneously control the complete film SOR of the deposition process to a desired level and minimize the variance of the partial film SOR. State feedback controllers are considered in this work, i.e., the values of the complete film SOR and of the partial film SOR are assumed to be available for feedback control. Such measurements may be obtained in real-time through a combination of real-time gas phase measurements and empirical models that predict film porosity from gas phase measurements.

A. Regulation of complete film site occupancy ratio

Since the film porosity is the main control objective in this work, we first consider the problem of regulation of the expected complete film SOR to a desired level, ρ_{set}, within a model predictive control framework. The substrate temperature is used as the manipulated input and the deposition rate is fixed at a certain value, W_0, during the entire closed-loop simulation. To account for a number of practical considerations, several constraints are added to the control problem. First, there is a constraint on the range of variation of the substrate temperature. This constraint ensures validity of the on-lattice kMC model. Another constraint is imposed on the rate of change of the substrate temperature to account for actuator limitations. We note that classical control schemes like proportional-integral (PI) control cannot be designed to explicitly account for input/state constraints, optimality considerations and the batch nature of the deposition process, and thus, their use will not be pursued in this work.

The control action, at a time t and state ρ, is obtained by solving a finite-horizon optimal control problem. The optimal temperature profile is calculated by solving a finite-dimensional optimization problem in a receding horizon fashion. Specifically, the MPC problem is formulated based on the deterministic ODE of Eq.6 as follows:

$$\begin{aligned}
&\min_{T_1,\ldots,T_i,\ldots,T_p} J(\rho(t)) = \sum_{i=1}^{p} q_{sp,i}\left[\rho_{set} - \langle \rho(t+i\Delta)\rangle\right]^2 \\
&\text{subject to} \\
&\langle \rho(t+i\Delta)\rangle = \rho^{ss}(T_i,W_0) \\
&\quad + \left(\langle \rho(t+(i-1)\Delta)\rangle - \rho^{ss}(T_i,W_0)\right) e^{-\Delta/\tau(T_i,W_0)} \\
&T_{min} < T_i < T_{max}, \left|T_{i+1}-T_i\right|/\Delta \le L_T, i = 1,2,\ldots,p
\end{aligned} \tag{18}$$

where t is the current time, Δ is the sampling time, p is the number of prediction steps, $p\Delta$ is the specified prediction horizon, T_i, $i = 1, 2, \ldots, p$, is the substrate temperature at the ith step ($T_i = T(t+i\Delta)$), respectively, W_0 is the fixed deposition rate, $q_{sp,i}$, $i = 1, 2, \ldots, p$, are the weighting penalty factors for the error of the complete film SOR at the ith prediction step, T_{min} and T_{max} are the lower and upper bounds on the substrate temperature, respectively and L_T is the limit on the rate of change of the substrate temperature. In the MPC formulation of Eq.18, J is the cost function, which contains penalty on the squared difference between the desired value of the complete film SOR, ρ_{set}, and the predicted values of this variable at all time steps.

The dynamics of the expected value of the complete film SOR are described by the deterministic first-order ODE of Eq.8. The dependence of model parameters on process parameters is obtained from the parameter estimation at a variety of conditions. Due to the availability of analytical solutions of the linear ODE model of Eq.8, these analytical solutions can be used directly in the MPC formulation of Eq.18 for the prediction of $\langle \rho(t)\rangle$. The system state, $\rho(t)$, is the complete film SOR at time t. Note that $\rho(t)$, which is obtained directly from the simulation in real-time, is considered as the expected complete film SOR and can be used as an initial condition for the solution of the deterministic ODE of Eq.8. In the closed-loop simulations, the instantaneous values of ρ and ρ_p are made available to the controller at each sampling time; however, no statistical information, e.g., the expected value of complete/partial film SOR, is available for feedback. The optimal set of control actions, (T_1, T_2, $\ldots$, T_p), is obtained from the solution of the multi-variable optimization problem of Eq.18, and only the first value of the manipulated input trajectory, T_1, is applied to the deposition process during the time interval $(t, t+\Delta)$. At time $t+\Delta$, a new measurement of ρ is received and the MPC problem of Eq.18 is solved for the next control input trajectory.

B. Fluctuation regulation of partial film site occupancy ratio

Reduction of run-to-run variability is another goal in process control of a thin film growth process. In this work, the fluctuation of film SOR is represented by the variance of partial film SOR, $\mathrm{Var}(\rho_p)$. Ideally, a zero value means no fluctuation from run to run. However, it is impossible to achieve zero variance of partial film SOR due to the stochastic nature of the thin film growth process. Thus, the control objective of fluctuation regulation is to minimize the variance by manipulating the process parameters.

In this work, the fluctuation is included into the cost function together with the error of the complete film SOR. Specifically, the MPC formulation with penalty on the error of the expected complete film SOR and penalty on the variance of the partial film SOR is given as follows:

$$\begin{aligned}
&\min_{T_1,\ldots,T_i,\ldots,T_p} J(\rho(t)) = \\
&\sum_{i=1}^{p} \left\{ q_{sp,i}\left[\rho_{set} - \langle \rho(t+i\Delta)\rangle\right]^2 + q_{var,i}\mathrm{Var}[\rho_p(t+i\Delta)] \right\} \\
&\text{subject to} \\
&\langle \rho(t+i\Delta)\rangle = \rho^{ss}(T_i,W_0) \\
&\quad + \left(\langle \rho(t+(i-1)\Delta)\rangle - \rho^{ss}(T_i,W_0)\right) e^{-\Delta/\tau(T_i,W_0)} \\
&\mathrm{Var}(\rho_p(t+i\Delta) = \mathrm{Var}_p^{ss}(T_i,W_0) \\
&+ \left(\mathrm{Var}\left[\rho_p(t+(i-1)\Delta)\right] - \mathrm{Var}_p^{ss}(T_i,W_0)\right) e^{-\Delta/\tau_p(T_i,W_0)} \\
&T_{min} < T_i < T_{max}, \left|T_{i+1}-T_i\right|/\Delta \le L_T, i = 1,2,\ldots,p
\end{aligned} \tag{19}$$

where $q_{sp,i}$ and $q_{var,i}$, $i = 1, 2, \ldots, p$, are weighting penalty factors on the error of the complete film SOR and of the variance of the partial film SOR, respectively. Other variables in Eq.19 are defined similarly to the ones in Eq.18. The same constraints as in Eq.18 are imposed on the MPC formulation of Eq.19. Due to the unavailability of statistical information of the partial film SOR in real-time, the initial condition of the partial film SOR is regarded as a deterministic variable and the initial condition at $t = 0$ for $\text{Var}(\rho_p(t))$ is considered to be zero in the MPC formulation.

V. Simulation results

In this section, open-loop simulations of the kMC model of a silicon thin film growth process using the methodology described in Section II are presented. The data obtained from the open-loop simulations of different conditions are used as the basis for parameter estimation. Model predictive controllers of Eqs.18 and 19 are applied to the thin film growth process to simultaneously control the complete film SOR of the deposition process to a desired level and minimize the variance of the partial film SOR.

A. Open-loop simulations

In this subsection, the thin film deposition process is simulated according to the algorithm described in section II. The evolution of complete film SOR and the variance of partial film SOR are computed from Eqs.3 and 5, respectively. The lattice size L is equal to 100 throughout this work. The choice of lattice size is determined from a balance between statistical accuracy and reasonable requirements for computing power. Dependence of film porosity on the lattice size has been discussed in [8], [9]. 1000 independent simulation runs are carried out to obtain the expected value and the variance of the film SOR. The simulation time is 1000 s. All simulations start with an identical flat initial condition, i.e., only a substrate layer is present on the lattice without any deposited particles.

Fig.3 shows the evolution profile of the mean value of the complete film SOR and the variance of the partial film SOR during the deposition process for the following process parameters: $T = 600$ K and $W = 1$ layer/s. In Fig.3, the film SOR is initially 0 and as particles begin to deposit on the film, the film SOR increases with respect to time and quickly reaches a steady-state value. The top 100 layers are chosen in the calculation of the partial film SOR, i.e., $H_p = 100$ in Eq.4. Snapshots of the thin film microstructure at different times, $t = 100$ s, 400 s, 700 s and 1000 s, of the open-loop simulation are shown in Fig.4.

B. Closed-loop simulations

In this section, the model predictive controllers of Eqs.18 and 19 are applied to the kMC model of the thin film growth process described in section II. The dependence of the model parameters on the substrate temperature is obtained using the parameter estimation described in subsection III-C on the basis of the open-loop simulation data.

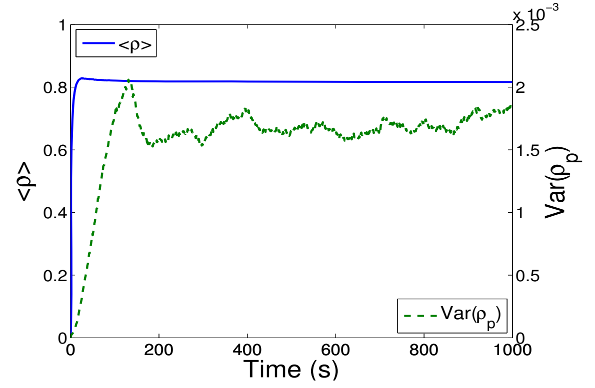

Fig. 3. Mean value of the complete film SOR (solid line) and variance of the partial film SOR (dashed line) versus time for a 1000 s open-loop deposition process with substrate temperature $T = 600$ K and deposition rate $W = 1$ layer/s.

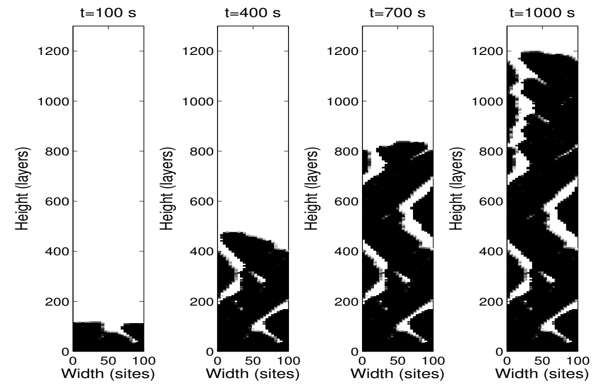

Fig. 4. Snapshots of the film microstructure at $t = 100$ s, 400 s, 700 s and 1000 s of the open-loop deposition process with substrate temperature $T = 600$ K and deposition rate $W = 1$ layer/s.

In the closed-loop simulation, the value of the substrate temperature is obtained from the solution of the problem of Eqs.18 and 19 at each sampling time and is applied to the closed-loop system until the next each sampling time. The complete film SOR and the partial film SOR are obtained directly from the kMC model of the thin film at each sampling time as the state of the system and are fed into the controller. The sampling time is fixed in all closed-loop simulations to be $\Delta = 5$ s, which is in the same order of magnitude of the time constant of the dynamics of the complete film SOR, τ. The optimization problems in the MPC formulations of Eqs.18 and 19 are solved using a local constrained minimization algorithm.

The constraint on the rate of change of the substrate temperature is imposed onto the optimization problem, which is realized in the optimization process in the following way:

$$T_i - L_T\Delta \leq T_{i+1} \leq T_i + L_T\Delta, \quad i = 1,2,3,4, \text{ and } 5. \quad (20)$$

The desired value (set-point) for the complete film SOR in the closed-loop simulations is 0.9. The number of prediction steps is 5. The deposition rate is fixed at 1 layer/s and all closed-loop simulations are initialized with an initial

temperature of 300 K. The maximal rate of change of the temperature is 10 K/s. Expected values and variances are calculated from 1000 independent simulation runs.

1) Regulation of complete film site occupancy ratio: First, the closed-loop simulation results of complete film SOR regulation using the model predictive control formulation of Eq.18 are provided. In this MPC formulation, the cost function contains only penalty on the difference of the complete film SOR from the set-point value. Specifically, the optimization problem is formulated to minimize the difference between the complete film SOR set-point and the prediction of the expected complete film SOR at the end of each prediction step. All weighting penalty factors, $q_{sp,i}$, $i = 1, 2, \ldots, 5$, are assigned to be equal. Fig.5 shows the profiles of the expected value of the complete film SOR in the closed-loop system simulation. The profiles of the complete film SOR and of the substrate temperature from a single simulation run are also included in Fig.5.

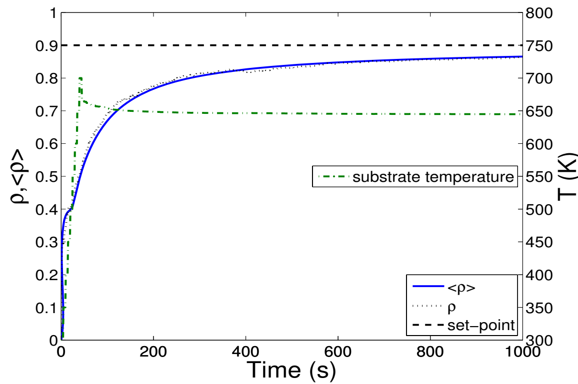

Fig. 5. Closed-loop profiles of the complete film SOR (solid line) and of the expected value of the complete film SOR (dotted line) under the controller of Eq.18. The profile of the substrate temperature is also included (dash-dotted line).

In Fig.5, the substrate temperature increases linearly at the initial stages due to the constraint on the rate of change, and it approaches to a value around 650 K, which is calculated from the optimization problem based on the current complete film SOR. The expected complete film SOR reaches the value of 0.87 at the end of the simulation. There is a difference of 0.03 from the set point, which is due to the fact that the first-order ODE model is not an exact description of the film SOR dynamics, but rather an approximation. However, for the purpose of control design, the first-order ODE model is acceptable. Another reason for the difference is the cumulative nature of the complete film SOR. Since the initial temperature, 300 K, is far below the optimal temperature for the desired film SOR, it takes some time for the substrate temperature to reach the optimal temperature. The initial condition of the substrate temperature results in a period of low temperature at the initial stages. In this period, layers with higher porosity are deposited onto the film and, as a result, the complete film SOR is lowered. Thus, it takes longer time for the complete film SOR to reach its steady-state value. The difference between the set-point and the closed-loop steady-state value can be overcome by pre-setting a higher initial substrate temperature. Another possible method to improve the closed-loop performance is to replace the quadratic cost function that penalizes the deviation of the SORs from the desired values with other functions, since quadratic terms slow down the convergence speed in the vicinity of the set point. Snapshots of the film microstructure at different times, $t = 100$ s, 400 s, 700 s and 1000 s, of the closed-loop simulation are shown in Fig.6.

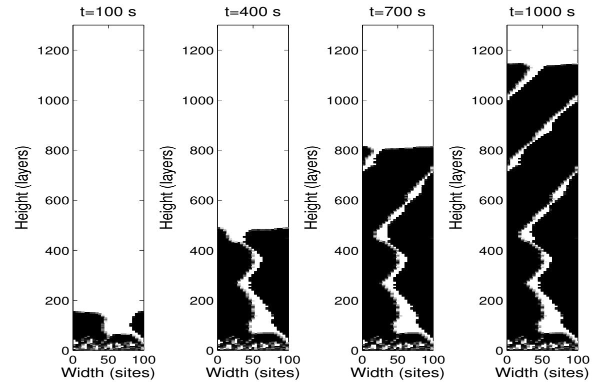

Fig. 6. Snapshots of the film microstructure at $t = 100$ s, 400 s, 700 s and 1000 s of the closed-loop simulation under the feedback controller of Eq.18 with $q_{sp,i} = 1$, $i = 1,2,3,4,$ and 5.

2) Fluctuation regulation of partial film site occupancy ratio: To reduce the run-to-run variability of the film porosity, the variance of the partial film SOR is added into the cost function in the model predictive controller of Eq.19. There are two weighting factors, $q_{sp,i}$ and $q_{var,i}$, which represent the weights on the complete film SOR and on the variance of the partial film SOR prediction, respectively. Fig.7 shows the profiles of the expected complete film SOR and of the substrate temperature in the closed-loop simulation, with the following values assigned to the weighting factors:

$$q_{sp,i} = 1, \quad q_{var,i} = 10, \quad i = 1,2,3,4, \text{ and } 5. \qquad (21)$$

As shown in Fig.7, the complete film SOR and the substrate temperature evolve similarly as in Fig.5. However, with the cost function including penalty on the variance of the partial film SOR, the optimal temperature is higher than the one in Fig.5, since a higher substrate temperature is in favor of decreasing run-to-run fluctuations. Fig.8 shows a comparison of the variance of the partial film SOR between the two model predictive controllers with $q_{var,i} = 0$ and $q_{var,i} = 10$, $i = 1,2,3,4,$ and 5. It can be seen that the variance of the partial film SOR is lowered with penalty on this variable included into the cost function of the MPC formulation. Snapshots of the film microstructure at different times, $t = 100$ s, 400 s, 700 s and 1000 s, of the closed-loop simulation are shown in Fig.9.

VI. Conclusions

In this work, a model predictive controller was developed to regulate film porosity and minimize its fluctuation in

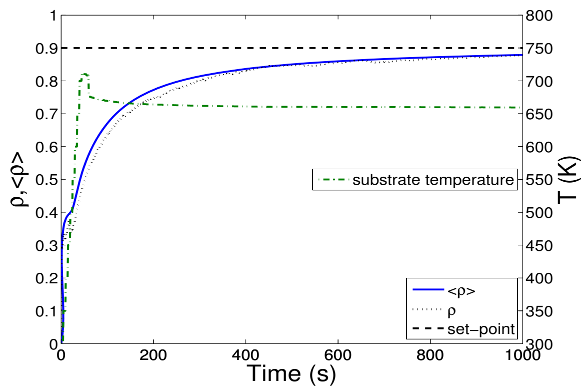

Fig. 7. Closed-loop profiles of the complete film SOR (solid line) and of the expected value of the complete film SOR (dotted line) under the controller of Eq.19. The profile of the substrate temperature is also included (dash-dotted line).

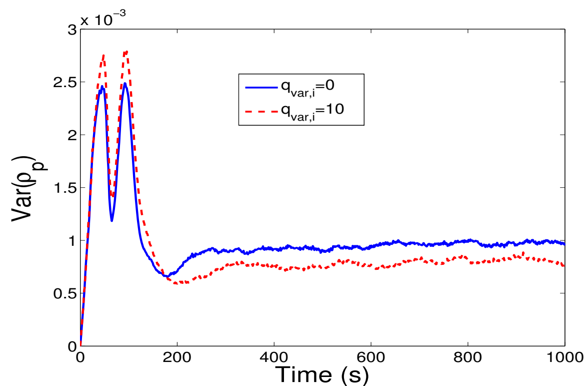

Fig. 8. Comparison of the variance of the partial film SOR for different weights: $q_{var,i} = 0$ (solid line) and $q_{var,i} = 10$ (dashed line).

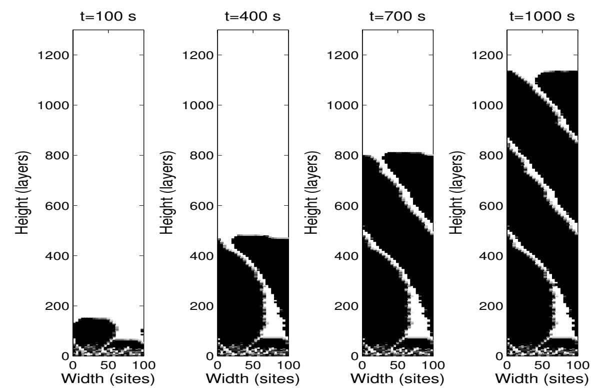

Fig. 9. Snapshots of the film microstructure at $t = 100$ s, 400 s, 700 s and 1000 s of the closed-loop simulation under the feedback controller of Eq.19 with $q_{sp,i} = 1$, $q_{var,i} = 10$, $i = 1,\ldots,5$.

thin film deposition modeled via a triangular lattice-based kMC simulator. Appropriate definitions of film SOR and its fluctuation were introduced to describe film porosity. Deterministic and stochastic ODE models were derived that describe the time evolution of film SOR and its fluctuation. The developed ODE models were used as the basis for the design of MPC algorithms that include penalty on the film SOR and its variance to regulate the expected value of film SOR at a desired level and reduce run-to-run fluctuations.

References

[1] K. J. Åström. *Introduction to Stochastic Control Theory*. Academic Press, New York, 1970.

[2] P. D. Christofides, A. Armaou, Y. Lou, and A. Varshney. *Control and Optimization of Multiscale Process Systems*. Birkh*ä*user, Boston, 2008.

[3] R. Cuerno, H. A. Makse, S. Tomassone, S. T. Harrington, and H. E. Stanley. Stochastic model for surface erosion via ion sputtering: Dynamical evolution from ripple morphology to rough morphology. *Physical Review Letters*, 75:4464–4467, 1995.

[4] S. F. Edwards and D. R. Wilkinson. The surface statistics of a granular aggregate. *Proceedings of the Royal Society of London Series A - Mathematical Physical and Engineering Sciences*, 381:17–31, 1982.

[5] K. A. Fichthorn and W. H. Weinberg. Theoretical foundations of dynamical Monte Carlo simulations. *Journal of Chemical Physics*, 95:1090–1096, 1991.

[6] D. T. Gillespie. A general method for numerically simulating the stochastic time evolution of coupled chemical reactions. *Journal of Computational Physics*, 22:403–434, 1976.

[7] G. Hu, Y. Lou, and P. D. Christofides. Dynamic output feedback covariance control of stochastic dissipative partial differential equations. *Chemical Engineering Science*, 63:4531–4542, 2008.

[8] G. Hu, G. Orkoulas, and P. D. Christofides. Modeling and control of film porosity in thin film deposition. *Chemical Engineering Science,* accepted, 2009.

[9] G. Hu, G. Orkoulas, and P. D. Christofides. Stochastic modeling of film porosity in thin film deposition. In *Proceedings of American Control Conference,* in press, St. Louis, MO, 2009.

[10] S. Keršulis and V. Mitin. Monte carlo simulation of growth and recovery of silicon. *Matetial Science & Engineering B*, 29:34–37, 1995.

[11] G. Kloster, T. Scherban, G. Xu, J. Blaine, B. Sun, and Y. Zhou. Porosity effects on low-k dielectric film strength and interfacial adhesion. In *Interconnect Technology Conference, 2002. Proceedings of the IEEE 2002 International*, pages 242–244, 2002.

[12] S. W. Levine and P. Clancy. A simple model for the growth of polycrystalline Si using the kinetic Monte Carlo simulation. *Modelling and Simulation in Materials Science and Engineering*, 8:751–762, 2000.

[13] Y. Lou and P. D. Christofides. Estimation and control of surface roughness in thin film growth using kinetic Monte-Carlo models. *Chemical Engineering Science*, 58:3115–3129, 2003.

[14] Y. Lou and P. D. Christofides. Feedback control of growth rate and surface roughness in thin film growth. *AIChE Journal*, 49:2099–2113, 2003.

[15] Y. Lou and P. D. Christofides. Feedback control of surface roughness using stochastic PDEs. *AIChE Journal*, 51:345–352, 2005.

[16] Y. Lou and P. D. Christofides. Nonlinear feedback control of surface roughness using a stochastic PDE: Design and application to a sputtering process. *Industrial & Engineering Chemistry Research*, 45:7177–7189, 2008.

[17] Y. Lou, G. Hu, and P. D. Christofides. Model predictive control of nonlinear stochastic partial differential equations with application to a sputtering process. *AIChE Journal*, 54:2065–2081, 2008.

[18] P. B. Maksym. Fast Monte Carlo simulation of MBE growth. *Semiconductor Science and Technology*, 3:594–596, 1988.

[19] D. Ni and P. D. Christofides. Multivariable predictive control of thin film deposition using a stochastic PDE model. *Industrial & Engineering Chemistry Research*, 44:2416–2427, 2005.

[20] A. Varshney and A. Armaou. Multiscale optimization using hybrid PDE/kMC process systems with application to thin film growth. *Chemical Engineering Science*, 60:6780–6794, 2005.

[21] D. D. Vvedensky, A. Zangwill, C. N. Luse, and M. R. Wilby. Stochastic equations of motion for epitaxial growth. *Physical Review E*, 48:852–862, 1993.

[22] L. Wang and P. Clancy. A kinetic Monte Carlo study of the growth of Si on Si(100) at varying angles of incident deposition. *Surface Science*, 401:112–123, 1998.

[23] L. Wang and P. Clancy. Kinetic Monte Carlo simulation of the growth of polycrystalline Cu films. *Surface Science*, 473:25–38, 2001.